Journal of The Electrochemical Society, **161** (12) A1772-A1776 (2014)
0013-4651/2014/161(12)/A1772/5/$31.00 © The Electrochemical Society

The Cycling Performance and Surface Passivation Qualities of a Heterogeneous Amorphous Ni_xSiO_y/Polycrystalline $NiSi_2$ Core Shell Nanowire Used as a Li-Ion Battery Anode

Isaac N. Lund,[a,b,z] Jae Ho Lee,[a,b] Harry Efstathiadis,[a] Pradeep Haldar,[a] and Robert Geer[a]

[a]*State University of New York, College of Nanoscale Science and Engineering, Albany, New York 12203, USA*
[b]*Battery Energy Storage System -Technologies, Albany, New York 12208, USA*

The cycling stability and the surface passivation qualities of a heterogeneous polycrystalline $NiSi_2$/amorphous Ni_xSiO_y core-shell nanowires cycled in a Li ion half cell is reported. The nanowire morphology showed stable cycling and excellent charge rate capability having a stable capacity above 1700 mAh/g when cycled in a coin cell at 1/2 C and retaining a capacity of 300 mAhr/g when cycled at a 10 C charge rate. It is shown that the stable cycling is due to the passivation qualities of the oxide components within the amorphous shell which create a stable solid-electrolyte interphase (SEI) during charging which is reduced during discharging through the conductive pathway provided by the Ni doping in the shell and $NiSi_2$ in the core. The $NiSi_2$ core interacts with Li through intercalation retaining its rigid core even while Li charged, the overall dimensions of the structure mitigate any pulverization issues, and the conductive core along with the Ni doping disallow any Li trapping leading to high columbic efficiency.

Manuscript submitted May 7, 2014; revised manuscript received July 30, 2014. Published August 12, 2014.

Lithium-ion (Li-ion) batteries are the energy storage devices of choice for items ranging from portable electronic devices to electric vehicles (EVs). Most current batteries in this technology family rely on graphite as an anode material, which has relatively low charge storage capacity inhibiting the range of electric vehicles and the life-time of portable electronics. The use of higher capacity materials for both anode and cathode can alleviate the life-time problems, but are plagued by an array of issues resulting from the materials having an alloying rather than an intercalation reaction with Li.[1–7] For anode materials Si has the highest theoretical capacity (4422 mAh/g 11X higher than graphite at 372 mAh/g) and has been sought after for use in Li-ion batteries.[1–5] Utilizing Si as an anode material creates three different problems in its application namely: pulverization created through strain in volume expansion during alloying, Li trapping due to Si semiconductor to conductor transition when lithiated, and unmitigated creation of a passivation layer on the anode called solid-electrolyte interphase (SEI) growth.[1–8] The SEI is formed due to the bath constituents being unstable at the operating voltage of the Li-ion battery thus decomposing into an insulating layer on the electrode surface.[1–7] Since Si goes through continuous volume expansion during lithiation, Si brings new unpassivated material to the electrode surface to be passivated creating a large SEI layer.[1–8]

For Si to achieve such a high capacity Si alloys with Li to create the $Li_{22}Si_5$ silicide causing a 400% volume expansion during the reaction.[1–4] The strain induced pulverization however was shown to be mitigated by going to nano dimensioned materials namely under 150 nm.[6] The second problem in the creation of an unstable SEI passivation layer however has not been solved for Si.[1–5] This passivation layer is created upon the first several cycles of the Si anode material with the electrolyte and is mainly comprised of Si alkyl carbonate compounds, lithium silicates (LixSiOy) and lithium fluoride (LiF).[5,7–9] Si has been shown to become unreactive to Li when given an alkyl (methane) or siloxane end termination.[7] Both the lithium silicates and the alkyl carbonate SEI components would satisfy this condition with the LiF being weakly bound to the SEI components.[7–9] Another problem with the application of Si is Li trapping as described by Kasavajula, where discharging is a surface dominated process and the insulating properties of Si can trap Li inside the bulk of the material by breaking a conductive pathway for Li to the electrolyte.[8]

In this work we are utilizing a heterogeneous $NiSi_2/Ni_xSiO_y$ core-shell nanowire with the growth description and initial electrochemical cycling performance shown in a previous manuscript.[10] The previously reported results displayed the unique growth of a heterogeneous $NiSi_2/Ni_xSiO_y$ core-shell nanowire when tested in a full cell geometry was stable at a capacity of 1727 mAh/g for 90 cycles.[10] Our intent through this manuscript is to discuss the methods for surface stability, capacity degradation effects, and to display longer term cycling results.

Experimental

We utilized novel heterogeneous nanowires consisting of a multicrystalline $NiSi_2$ inner core and an amorphous Ni_xSiO_y outside shell. The nanowires were grown by metal induced growth process directly onto a 304 stainless steel substrate with a modified metal induced growth process that is described in a previous manuscript.[10] For electrochemical analysis we grew the nanowires directly onto a stainless steel substrate since interdiffusion of Ni and Fe is negligible at the nanowire deposition temperature and it makes integration into a battery application straight forward. There is no slurry formation or mixing with carbon black or binder. This is done to translate the high surface area electrode material into improved cycle life and charge rate capability, and to avoid the problems of adhesion between active Si material and binders which is a tenuous relationship.[7,8] The current active material loading is determined from the difference of the weights before and after nanowire deposition and for the tested samples sits at .1 mg/cm^2.

For ease of analysis of the nanowire samples in different charge states, cyclic voltammetry (CV) was performed on the anode in a half cell setup constructed inside a reaction flask using a Pine Wavenow potentiostat. In a half cell format, the cathode and reference electrode material were the same (Li wire) and the electrolyte used was a 1M mixture of lithium hexafluorophosphate ($LiPF_6$, Sigma Aldrich) in a 1:1 ethylene carbonate, diethyl carbonate (EC:DEC, Sigma Aldrich) solution. The electrodes were connected to the potentiostat by alligator clips and the electrodes were draped into the electrolyte bath. The half cell was manufactured and tested inside a Vacuum Atmospheres glove box in a reaction flask with 3 top dip tubes; the flask tops were covered with press seal Parafilm to minimize evaporation effects. The samples were cycled for 90 cycles from 2.5–0.01 V to ensure sufficient SEI production and any phase and morphological changes would have taken place. The samples labeled post Li and surface rinse were completely discharged in CV to 2.5 V. The surface rinse samples were completely discharged and treated by rinsing the samples gently with DEC and placed along with the post Li sample to allow it to dry in the glove box overnight. The Li charged samples are stopped in the CV at 0.01 V and left in the glove box to dry off any excess liquid electrolyte overnight. Four samples are investigated in this work: a) as deposited nanowires, b) Li charged nanowires, c) post Li fully discharged nanowires, and d) surface rinsed post Li fully discharged nanowires.

[z]E-mail: ilund@albany.edu

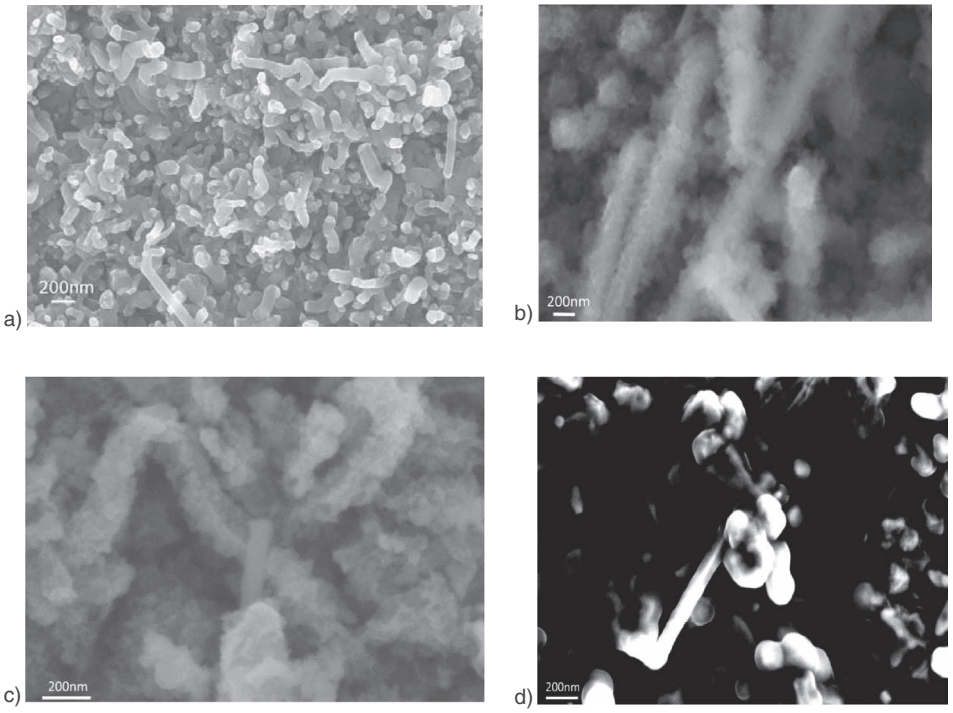

Figure 1. SEM micrographs of heterogeneous nanowires shown in a) as deposited, b) Li-charged, c) post Li cycled, and d) DEC surface rinsed.

The morphology of the heterogeneous nanowires was investigated in LEO 1550 scanning electron microscope (SEM) with an accelerating voltage of 4 KeV with cross-sectional morphology imaged by a JEOL 2010F transmission electron microscope (TEM) with a 300 KeV accelerating voltage. To determine the phase changes that occur during different states of lithiation Raman spectroscopy was taken through a Horiba confocal Raman spectrometer. Attenuated total reflectance Fourier transform infra-red (ATR-FTIR) spectroscopy was performed with a Bruker Tensor 27 system using a sampling length of 800–4000 cm^{-1} on samples in multiple different conditions to probe the SEI interface and its retention onto the nanowires surface. The ATR-FTIR tested samples were: blank stainless steel reference sample, as grown nanowire samples, and samples after Li cycling that have had and have not had a surface rinse as described previously. The TEM samples were prepared by sonicating a nanowire sample in an isopropyl alcohol (IPA) solution for a period of 5 minutes and then 5 drops of the solution were dropped onto a holy carbon film on a Cu TEM grid and let dry in air before placing into the TEM. For the post Li TEM sample we expected the sample preparation step to completely break-off the SEI layer.

Results and Discussion

The SEM micrographs of the nanowire morphology through its different lithium charged conditions are shown in Figure 1, a) as deposited nanowires, b) the Li charged nanowires, c) the post Li nanowires, and d) is the surface rinsed nanowires.[7] The SEM micrographs in a) show the nanowires are around 80 nm in diameter and around 1 μm long, the nanowires in b) show a retention of their structure during charging due to $NiSi_2$ core only reacting with Li through and intercalation reaction thus not losing structural rigidity during Li charging, in c) we observe that when discharged the nanowire retains its structure and obtains a rough surface coating compliant with SEI formation, and d) after the surface rinse we observe the removal of the rough surface coating that is consistent with SEI production.[7,8] This analysis shows two keys things: first that the structure of the nanowires are maintained even when Li charged which keeps it from agglomerating like other nanowire solutions, and second that the SEI is either partially or completely rinsed away by the DEC rinse.[7,8,11]

The retention of the structure is also shown through the TEM analysis as shown in Figure 2. The as deposited nanowire is shown in Figure 2a) showing the previously shown core-shell morphology.[10] The post Li cycled sample as shown in Figure 2b) shows that the outside amorphous shell has gotten less dense during the Li charging and discharging. This would be due to the Li alloying during charging, which causes the amorphous shell to expand without a complete contraction during discharging which would explain the increase in capacity during the first several cycles as shown in the previous paper by providing a pathway for Li to react with more Si in the nanowire shell.[10] Also shown in Figure 2b) is the loss of the conformity in the amorphous shell which could be due to loss of active material either during Li cycling or in the TEM sample preparation process. The loss of material would be less likely at higher charging rates since Li would diffuse into less material in the amorphous shell creating less expansion and a lower likelihood of active material isolation creating overall a more stable cycling as shown in the higher rate capacity cycling in supplementary figure S1.

To check the phase of the nanowire, and to determine the phase transitions over charging states Raman spectroscopy was taken of the samples mimicking the nanowire charged states in the SEM analysis. All of the samples are plotted on a single graph as shown in Figure 3 with the different spectrums artificially separated from one another. The spectrum for the as grown nanowire show a peak compliant with $NiSi_2$ at 371 cm^{-1} from the core, Si at 520 cm^{-1} from the amorphous shell and NiO at 1000 cm^{-1}.[10,12–17] The $NiSi_2$ occurs due

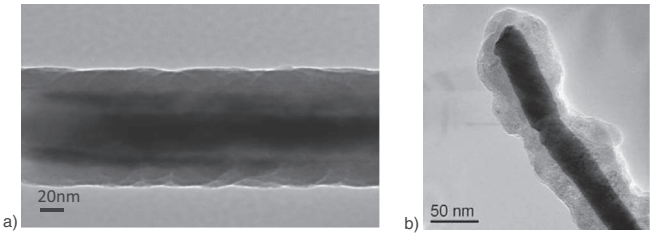

Figure 2. TEM micrographs of heterogeneous nanowire shown in a) the as deposited nanowire sample and b) nanowire post Li cycling with nanowire sample completely discharged

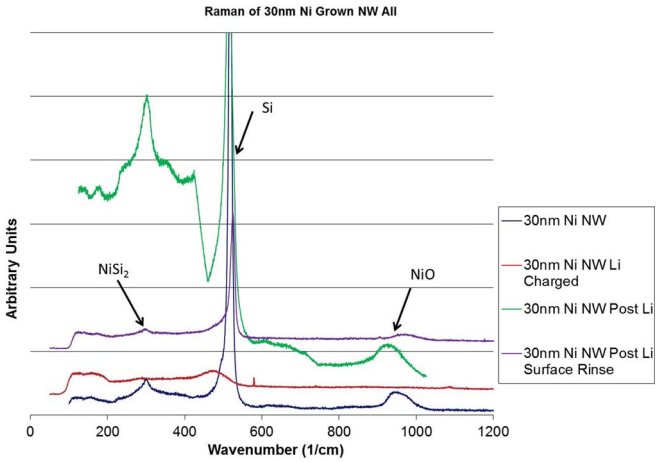

Figure 3. Raman spectroscopy heterogeneous nanowires in different stages of Li charging, with as deposited, Li charged, discharged and a surface rinsed sample all displayed on a single graph.

to the conservation of free Ni within the system when the Ni from the crystalline core diffuses into the amorphous shell doping it to 10 atomic%. The NiO signal shows that there is free Ni at the surface which needs to be passivated since NiO in the bulk would be reduced by any free Si.[18,19] The amount of free Ni on the surface should be the same as the solid solubility of Ni in Si determined by the phase diagram.[18,19] The Ni content is verified by XPS analysis shown in Table I, which is around 10% atomic percent of Ni, and thus we would expect the surface coating to have 10% NiO composition. The Raman spectrum for the Li charged nanowire sample shows the retention of the $NiSi_2$ which is consistent with the intercalation reaction, while the crystalline Si peak becomes a broad amorphous Si peak due to the Si amorphization process during lithiation, and the disappearance of the NiO occurs due to NiO splitting into its atomic components during lithiation creating Li_2O and Ni.[1–5,8,15–17] The Li_2O is an insulating compound commonly seen in the SEI components on graphite anode and is beneficial for nanowire stability throughout its charging cycle.[7,8] The post Li and surface rinsed spectrum show the reappearance of the original phases of the nanowires, which is consistent with that we see in the SEM analysis. The surface rinse sample shows a decrease in the NiO peak implying that some of the NiO species can be segregrated off and are not tightly bound to the nanowire surface. The reduction of NiO peak amplitude could explain the loss of conformity of the amorphous shell for the TEM post-Li cycling sample due to some of the NiO species being weakly bound to the nanowire structure and easily segregated off.

FTIR is taken of the samples to determine the components of the SEI species. Since the NiO component reversibly produces Li_2O on the surface of the anode, we expect any other SEI constituents to be weakly bound to the surface. As has been previously shown the main constituents of Si anode are carbonate decomposition products, lithium silicates, and Li-F components.[9] This occurs since the Si-O end termination is reduced by the carbonate based solvent and is replaced by alkyl carbonate end terminations on Si, blocking future lithium charging reactions.[7] The blocking of this decomposition pathway through the introduction of reaction displacement components (NiO) on the surface of Si creates a reversible SEI interface.[15–17] The FTIR analysis is shown in Figure 4 with the spectrum for the blank stainless steel substrate shown for background elimination. The as deposited nanowire sample shows a FTIR signal shows a signal only compliant with Si-O as expected in the amorphous shell. The Post Li sample displays multiple peaks that are compliant with carbonate decomposition products along with peaks compliant with silicon alkyl carbonate products.[7] The surface rinsed spectrum shows peaks compliant with Si-O showing that the silicon alkyl carbonate components are weakly bonded to the surface. This could be another way that the amorphous shell loses conformity when surface rinsed, by washing away SiO areas not shielded by NiO at the surface of the amorphous shell.

Table I. Composition of the as deposited nanowire, the nanowire post Li cycling, and the post Li cycled nanowire after a DEC surface rinse.

	Composition in atomic%						
Nanowire	Si	Ni	O	C	Li	F	P
30 nm Ni NW as grown	65	10	25	-	-	-	
30 nm Ni NW Post Li	3	6	17	19	25	28	2
30 nm Ni NW Surface Rinse	18	0	48	20	3	8	3

The FTIR spectrum shows that the silicon alkyl carbonate molecules are weakly bound to the nanowire surface leading to a mass loss decomposition pathway for silicon based anode by having them wash away.[7] However by incorporating a common reaction displacement anode surface (either NiO or Fe_2O_3) the silicon is shielded from the electrolyte and the alkyl carbonate end termination degradation pathway. To understand the amount of Ni doping in the surface of the nanowires and the constituents of the SEI, XPS surface scan was run on the as deposited nanowire sample, along with the post Li cycling sample, and surface rinse with the results tabulated in Table I. The as deposited shows a composition that is about 2:1 Si:O composition meaning a large portion but not all of the Si is oxidized, and 10% Ni contribution which is the solid solubility limit of Ni in Si.[18,19] The XPS analysis of the post Li cycled nanowires shows a large Li-F signal which is consistent with the Li-F constituents in the outside shell of the proposed Si SEI layer.[9] The surface rinse sample showed a decrease in the Li-F compositional signal showing that it is weakly bound to the outside of the SEI shell.[7–9] The C-O signal however increases due to the alkyl carbonate end terminations being intimately bound to any Si on the surface.[7–9] The NiO incorporated into the amorphous Si shell however provides a Li diffusion pathway to charge the whole structure instead of having the SEI Si alkyl carbonate components block the lithiation pathway.[7,15–17] To understand the thickness of the SEI the depth profiling was performed on the post Li sample by sputtering using an Ar+ ion beam with a beam energy of 1 kV and beam current of 0.5μA. Survey scans and high resolution scans of the Si 2p, Ni 2p C 1s, O 1s, F 1s, Li 1s, and P 2p energy spectra were taken of each sample to identify the compounds present on the surface. The result is shown in Figure S2 and through the calibration of the Ar^+ sputtering rate with a SiO_2 sample we get a sputter rate of 4 nm/min for our system. This translates into a measured SEI thickness of around 24 nm which is in the 20–50 nm thickness shown in literature but is an inaccurate measurement due to the SEI being an inhomogeneous layer.[1–8]

To understand the relationship of the SEI component to the added impedance of the system the nanowire samples were placed in a three terminal beaker cell and EIS measurements were run before and after 10 cycles between 2.5–0.01 V at a 0.5 C charge and discharge rate with the results shown in Figure 5. The EIS analysis is done in a three terminal beaker cell at a rate of 0.6 Hz and the analysis shows that the SEI component adds about 7 ohms of impedance to the Li diffusion pathway. The EIS of the "As Grown" nanowires shows a lower resistance than a normally utilized nanowire which is attributed to the added conductivity of the core-shell geometry.[1] The added resistance of the SEI formation as shown in the "Post Li" sample adds an amount of resistance that is double the original nanowire resistance which we attribute to the formation of alkyl carbonate compounds on the Si surface which acts as a Li blocking layer as discussed previously.[7,8]

To understand the gravimetric capacity as well as the cycling retention half cells were manufactured in a glove box and tested in a coin cell on an Arbin galvanostat between 2.5–0.01 V at room temperature. The voltage range was chosen to allow for complete reaction of Li into the $NiSi_2$ core which occurs through intercalation. After manufacturing the coin cells were allowed to sit for 3 hours

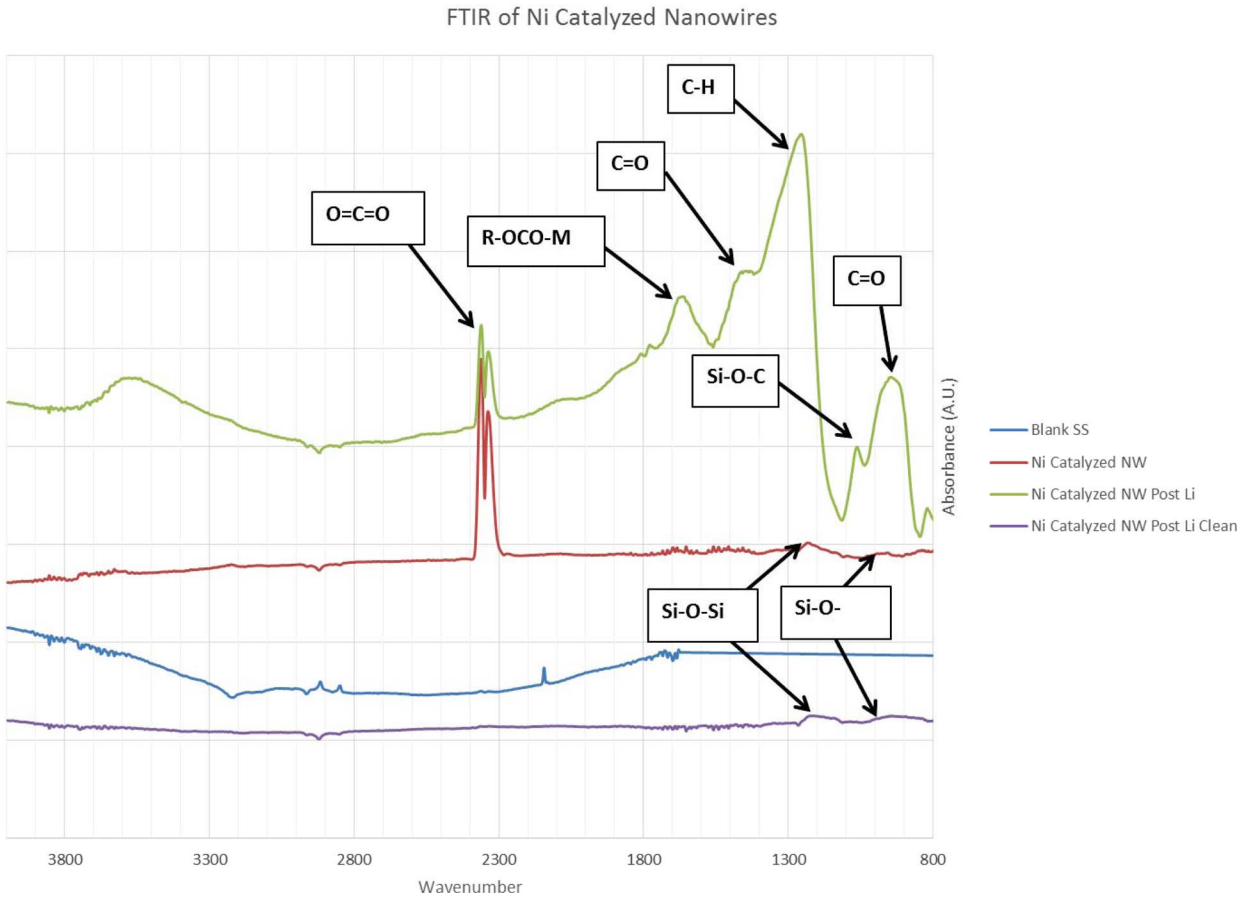

Figure 4. normalized ATR-FTIR results for nanowires in different stages of testing with labels for the characteristic organic peaks labeled on the graph.

to allow for complete electrode wetting before placing in chronopotentiometry testing. Figure 6 shows the chronopotentiometry testing of the nanowire anode when cycled at 0.5 C for 350 cycles. We observe that the initial capacity is above 1800 mAh/g which degrades in the first several cycles due to the setting up of the SEI layer as can be seen in the columbic efficiency mapped to the secondary y-axis. The capacity stabilizes at 1700 mAh/g for 150 cycles and then starts to slowly degrade hitting its 20% capacity retention mark after 300 cycles. The charge and discharge capacity track one another for a good columbic efficiency of 98–99% after the first several cycles. The loss in capacity is due to the loss of active material as explained above and shown in both the TEM and Raman analysis as shown in Figures 2 and 3. The capacity degradation during cycling should occur less at higher cycling rates due to smaller volume expansion in the outside shell allowing for more mass retention as shown in supplementary Figure S1. From the geometry of the nanowire we can obtain a theoretical capacity of about 2050 mAh/g for the structure, which

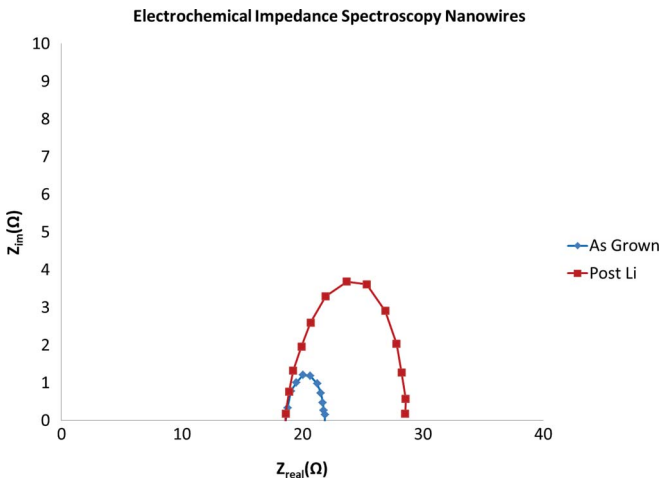

Figure 5. EIS measurements of a nanowire anode shown before and after 10 charge discharge cycles at 0.5 C rate.

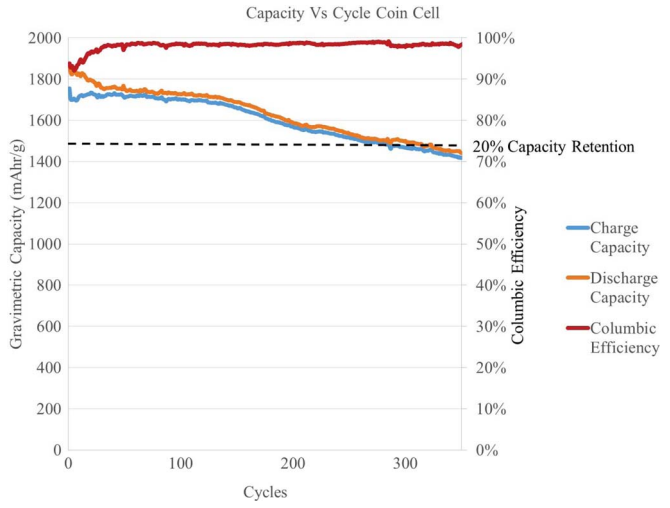

Figure 6. Cycling performance for half-cell in a coin cell cycled at 0.5 C rate for 350 cycles.

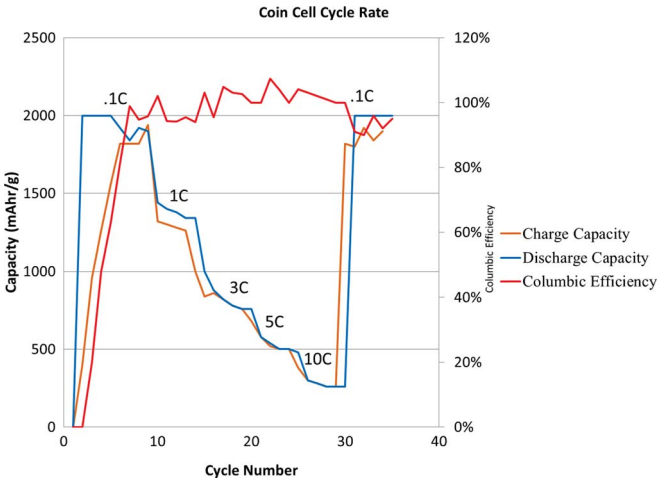

Figure 7. Cycle rate testing for a half cell in a coin cell cycled at rates between 0.1–10C.

is close to the initial measured capacity at 0.5 C of 1836 mAh/g. The nanowire has an overall diameter of 80 nm and an inside crystalline core diameter of 30 nm. The core is $NiSi_2$ which has a capacity of 600 mAh/g, and comprises 37.5% of the total composition. From the XPS analysis shown in Table I the shell is 45% Si at 4200 mAh/g, 45% SiO at 2600 mAh/g, and 10% Ni. This makes the compositional breakdown of the nanowire 37.5% $NiSi_2$, 28.125% Si, 28.125% SiO, and 6.25% Ni. From this calculation we obtain a theoretical capacity for the nanowire of 2050 mAh/g. The effect of electrode density and surface area should also assist with the life-time of the nanowire based sample, since the nanowires are grown directly onto the current collector and utilized without creating a slurry based anode the benefits of high surface area on cycle stability and charge rate capability would be directly translated into the electrochemical performance.

To understand how the highly surface nanostructured anode allows for higher charging rates the nanowire anode was placed into a coin cell and cycled at different charge rates between 0.1–10 C and at a voltage range 2.5–0.01 V, the results are shown in Figure 7. The charge rates step from 0.1 C up to 10 C and back to 0.1 C to show capacity retention at higher charging rates. The 0.1 C charge rate shows a capacity around 2000 mAh/g which is close to the theoretical capacity. The 1 C cycle rate is lower than 0.5 C by about 200 mAh/g. At higher C rates the capacity becomes less but still good with the gravimetric capacity of the nanowires at 10 C having the same capacity as commonly used graphite anode at 0.5C.[8] The gravimetric capacity is shown to completely recover when the cycle rate is stepped back to 0.1 C. The columbic efficiency is low during the first several cycles due to the setting up of the SEI layer but then sticks to around 100% with some variability due to noise in the instrument.

The good cycle rate performance of the nanowire anode as shown in Figure 7 is due to the high surface area of the nanowire based anode. Alloying based anode such as Si based anode are also less likely to degrade at higher cycle rates making this nanowire geometry more suitable for higher rate applications as shown in S1.[8] It is proposed that the stabilization of the nanowire cycling performance could be improved by incorporating an ex-situ deposited thicker reaction displacement coating over the nanowire to isolate the Si on the surface away from the alkyl carbonate end termination and decomposition pathway.

Conclusions

We have shown and thoroughly explained the surface reaction and the degradation mechanisms in the tested heterogeneous nanowire solution. This nanowire has high capacity while retaining good SEI characteristics due to the integration of reaction displacement anode material (NiO) on the nanowire surface. The NiO passivates the surface during lithiation and insulates Si from degrading by becoming passivated by alkyl carbonate end terminations. The nanowire anode is shown to have a capacity that is 6X higher than graphite anode that is stable for 300 cycles. The cycle rate shows that even at a high charge rate of 10 C the nanowire anode still retains a capacity of 300 mAh/g which is the tested gravimetric capacity of graphite at a 1 C rate. The nanowire recovers when switched from a high to a low cycle rate showing no fast charging rate degradation mechanism.

Acknowledgments

The writer acknowledges the support of New York State Energy Research Development Authority (NYSERDA) Advance Clean Power Technologies grant, and National Science Foundation (NSF) Partnership for Innovation grant.

References

1. C. K. Chan, R. Ruffo, S. S. Hong, and Y. Cui, *J. Power Sources*, **189**, 1132 (2009).
2. M. H. Park, M. G. Kim, J. Joo, K. Kim, J. Kim, S. Ahn, and J. Cho, *Nano Lett.*, **9**(11), 3844 (2009).
3. C. Yu, X. Li, T. Ma, J. Rong, R. Zhang, J. Shaffer, Y. An, Q. Liu, B. Wei, and H. Jiang, *Adv. Energy Mater.*, **2**, 68 (2010).
4. L. F. Cui, R. Ruffo, C. K. Chan, H. Peng, and Y. Cui, *Nano Letters*, **9**(1), 491 (2009).
5. Y. M. Lee, J. Y. Lee, H. T. Shim, J. K. Lee, and J. K Park, *J. the Electrochem. Soc.*, **154**, A515 (2007).
6. X. H. Liu, L. Zhong, S. Huang, S. X. Mao, T. Zhu, and J. Y. Huang, *ACS Nano*, **6**, 1522 (2012).
7. W. Xu, "Silicon Nanowire Anode For Lithium-Ion Batteries: Fabrication, Characterization and Solid Electrolyte Interphase" (Doctoral Thesis) (Doctoral Thesis) Chemical Engineering, Lousiana State University, (2011), Publication No. etd-05192011–103451.
8. U. Kasavajjula, C. Wang, and A. J. Appleby, *J. Power Sources* **163**, 1003 (2007).
9. M. Nie, D. P. Abraham,Y. Chen, A. Bose, and B. L. Lucht, *J. Phys. Chem.* **117**, 13403 (2013).
10. I. N. Lund, J. H. Lee, H. Efstathiadis, P. Haldar, and R. E. Geer, *J. Power Sources*, **246** 117 (2014).
11. W. Xu, Sri Sai S. Vegunta, and J. C. Flake, *J. Power Sources* **196**, 8583 (2011).
12. L. Wan, X. Zhang, B. Tang, Y. Ren, X. Cheng, D. Xu, H. Luo, and Y. Huang, *Thin Solid Films* **518**, 3646 (2010).
13. Y.-L. Jiang, A. Agarwal, G.-P. Ru, G. Cai, and B.-Z. Li, *Nucl. Instrum. Methods Phys. Res. B* **237**, 160 (2005).
14. W.-S. Lee, T.-H. Chen, C.-F. Lin, and J.-M. Chen, *Appl. Phys. A* **100**, 1089 (2010).
15. S. Y. Tan, C.-W. Chen, I-T. Chen, and C.-W. Feng, *Thin Solid Films* **517**, 1186 (2008).
16. X. Guo, H. Yu, Y.-L. Jiang, G.-P. Ru, D. W. Zhang, and B.-Z. Li, *Appl. Surf. Sci.* **257**, 10571 (2011).
17. F. F. Zhao, J. Z. Zheng, Z. X. Shen, T. Osipowicz, W. Z. Gao, and L. H. Chan, *Microelectron. Eng.* **71**, 104 (2004).
18. T. Shiozawa, "Improvement of Thermal Stability of Ni Silicide on Heavily Doped N+-Si" (Master's Thesis) Department of Electronics and Applied Physics, Tokyo Institute of Technology (2008) Publication No. 05M36269.
19. P. S. Lee, D. Mangelinck, K. L. Pey, J. Ding, J. Y. Dai, C. S. Ho, and A. See, "On the Ni–Si phase transformation with/without native oxide," *Microelectron. Eng.* **51–52**, 583 (2000).